Volume 66, Issue 1, 2022
Journal of Scientific Research
of
The Banaras Hindu University

Experimental investigations on Nano Titania - Polyacrylamide Composite Films

G.Veena [1] and Blaise Lobo[*2]

[1]Department of Physics, Karnatak University's KSCD, Dharwad, Karnataka, India, gveena8b8@gmail.com
[*2]Department of Physics, Karnatak University's KSCD, Dharwad, Karnataka, India, blaise.lobo@gmail.com

Abstract: **TiO_2 nanoparticles (titania) filled polyacrylamide (PAM) based composite films were prepared by solution casting technique, with filler levels (FLs) varying from 0.0 up to 19.50 Wt%. Spectroscopic, thermal, and electrical properties of these composite films were experimentally studied. Optical studies revealed a decrease in optical band gap of TiO_2 NPs filled PAM composite with increase in titania NP content in the composite, and also showed the formation of intermediate bands due to formation of CTCs. Thermal studies revealed that TiO_2 NP filled PAM composite samples exhibited low value of T_g and improved thermal stability at low (0.02 and 0.4 Wt%) and moderate FLs. The samples were subjected to temperature dependent Direct current (DC) electrical measurements in the temperature range of 303K to 340K. Variable Range Hopping (VRH) model was used to analyze the data. Activation energy and mott parameters were determined from VRH model. Results revealed a decrease in activation energy for thermally stimulated mobility of charge carriers, and so the electrical conductivity increases at low FLs. SEM images revealed good dispersion of titania NPs in the polymeric (PAM) host material at low FLs (FL = 0.02 and 0.4 Wt%). EDS spectra indicated the existence of C, N, O, Ti elements as the constituents of the studied polymer composites.**

Index Terms: **EDS analysis, Optical studies, PAM-TiO_2 composite, Thermal analysis, VRH Model analysis.**

I. INTRODUCTION

Polymeric materials, due to their unrivalled properties of being highly flexible, easily processable and having low density are widely employed in the fabrication of flexible displays, capacitors and in various other energy storage applications (Li et al, 2018; Zhou & Jiang, 2020). But, most of the common polymeric materials have low ionic conductivity (Zulkifli, 2012; Zhao & Liu, 2010), and one of the methods which can be adopted to overcome this problem is to incorporate inorganic and ceramic fillers into the polymeric matrix. This results in the formation of a new polymer based composite material. In recent times, a large number of research reports have been devoted to characterizing and scrutinizing the nano-scale inclusions in traditional polymeric materials; such composite materials are prepared because of their potential applications in different areas (Shukla et al, 2021; Shameem et al, 2021; Hassan et al, 2021; Wang et al, 2021). The incorporation of nano-fillers into a polymer matrix results in an enhancement in physical properties of the resulting polymer composite even at very low levels of filler when compared to their bulk counterparts. When nano-sized inorganic fillers are used as polymer additives, they exhibit additional advantages due to modifications in reactivity and properties, due to the nano -size of the filler. The advancement in the field of nanotechnology has resulted in the use of nano-filler incorporated polymer composites as promising materials for the fabrication of electro-optical devices, solid state sensors, anti - corrosive coatings and electronic devices (Harb et al, 2020; Singh et al, 2020; Rajeh et al, 2020; Faupel et al, 2010). The enhancement in material properties of the nano-filler incorporated polymeric composite is due to their higher surface area to volume ratio, which results in significantly enhanced interaction between the filler nanoparticles (NPs) and polymer molecules in the host matrix, and also due to the quantum confinement effects, which becomes active in these materials at the nano-scale (Ayanoğlu & Doğan, 2020). In fact, a small amount of filler made up of NPs could be dispersed in large volumes of the polymeric host to achieve desired properties in the resultant composite material, without affecting its processability. Various nano-fillers can be introduced in the polymeric host in order to tailor the properties of these composite materials (Mai & Yu, 2006; Shrivastava et al, 2016; Kim et al, 2015). As the performance of any device using polymeric composite materials mainly depends on properties of the polymeric host material which has been used, the search for

[*]Corresponding Author

a suitable polymeric material, having good ionic conductivity, thermal, optical and mechanical properties is extensively being pursued by researchers.

Polyacrylamide (PAM) is a highly water soluble and water - absorbent (swellable) polymer, which is non - polar (non-ionic), non - toxic, bio - compatible and biologically inert (Awad et al, 2020). The bio - adhesive property of PAM is utilized in controlled drug delivery systems (Roy & Prabhakar, 2010). PAM is adopted for a variety of wet end applications; it is utilized for electrophoresis, water clarification (in order to flocculate solids in waste water), oil recovery and biomedical applications (Green et al, 2000; Wever et al, 2013, Gavrilin, 2001). The structure and physical properties of PAM based materials are widely studied. The presence of the amide (-$CONH_2$) group enables hydrogen bonding of PAM with its component additives. A polymeric nano-composite (NC) comprising of gold (Ag) NPs dispersed in PAM matrix has been studied (Bai et al, 2007), wherein these researchers have reported that the formation of co-ordination bonds between the Ag NPs and PAM was responsible for the reduction and stabilization of the NPs incorporated in the polymeric host. A study reported the use of PAM - lithium chloride (LiCl) polymer electrolyte in electro - chemical capacitors; the material with 7.2 Wt % of LiCl in PAM exhibited a conductivity of 13.5 $\pm$4 mS cm^{-1}(Virya & Lian, 2017). Another study (Liu et al, 2021) demonstrated the use of PAM as electrolyte for the fabrication of a zinc battery. PAM based hydrogels are widely studied for sensor applications (Xie et al, 2020; Choudhary et al, 2020).

The electrical conductivity of a polymer composite depends on the movement of ions through the polymer matrix. The dense packing of polymer chains in a polymeric film due to crystallization hinders the free movement of smaller polymer chain segments. Therefore, the amorphous regions of a semi-crystalline polymeric material are involved in the movement of ions through the material, on the application of an electric field across the polymeric sample. A significant amount of research work has been done, focusing on enhancing the ionic conductivity, as well as the electro - chemical, mechanical and thermal stability of polymeric materials.

In order to enhance the structural, electrical and thermal properties of PAM, titanium dioxide (titania or TiO_2) NPs are used as the nano-filler. TiO_2 is a wide band gap semiconducting metal oxide which exists in three phases, namely, anatase, rutile and brookite. In the present case, anatase TiO_2 NPs are used, which have an optical band gap energy of 3.2 eV. These NPs are well known for their specific electronic properties, thermal and chemical stability. The anatase phase of titania is preferred over rutile phase, as the former is considered to be more efficient for applications involving enhanced electronic and charge transport properties (Hari et al, 2012; Ghosh et al, 2003). The incorporation of inorganic inert ceramic NPs such as titania (TiO_2) (Bahuleyan et al, 2019), silica (SiO_2) (Dhatarwal et al, 2020) and alumina (Al_2O_3) (Sankar et al, 2020) into a polymeric matrix inhibits the crystallization tendency of the polymer matrix and reduces its glass transition temperature (T_g). This leads to the enhancement of amorphousness in the resulting composite material, and consequently increases its ionic conductivity. The higher surface area of these nano - sized inorganic filler particles enables the increase in the effective interaction between these fillers and the polar groups present in the polymer structure. This interaction results in the formation of charge transfer complexes (CTCs) and create conducting pathways for the mobility of ions in the resulting composite material. Further, the addition of ceramic filler in a polymeric host also prevents polymer chain reorganization, which promotes ion transportation and decreases the inter-facial resistance of the material, resulting in enhancement of both the electro-chemical and mechanical stability of the polymer composite material. TiO_2 based polymer composites have been studied by various researchers, for use in various applications such as gas sensors and separators (Huyen et al, 2011; Ahmad et al, 2013), hybrid solar cells (Günes et al, 2008), photo - catalysts (Olad et al, 2012) and dye sensitized solar cells (Singh et al, 2010). Recent studies on TiO_2 based polymer electrolytes have revealed their effective use in diverse applications.

II. EXPERIMENTAL

A. Sample preparation

PAM of molecular mass 5,000,000 g/mol was procured from Himedia laboratories Pvt. Ltd., Mumbai. Spherical NPs of TiO_2, with average particle size of 65 nm were obtained from Ultra nanotech Private Limited, Bengaluru, India. Double distilled water was used as the solvent. Solution casting technique was used to obtain free standing films of PAM and TiO_2 NP filled PAM composite films. Appropriate amount (0.50 grams) of PAM was added in 200 ml of double distilled water (and stirred to be fully dissolved (for 24 hours) until a homogeneous and viscous liquid is obtained. This solution was filtered, and then it was poured into glass petridishes and kept for solvent evaporation in an air cooled, temperature controlled oven maintained at a temperature of 45°C for four days. The dried films were peeled off from the substrate to obtain pure PAM films.

In order to prepare the PAM-TiO_2 composite film, the required amount of TiO_2 NPs was dispersed in distilled water using an ultrasonicator; this dispersion (mixture) was then transferred to the glass beaker containing aqueous PAM solution. In fact, different measured volumes of the earlier prepared titania dispersed solution were added to aqueous PAM solution taken in different beakers, in order to obtain TiO_2 NP dispersed PAM solutions with different FLs. The mixture, in each case, was poured into a clean petridish and kept in an air cooled, temperature controlled oven maintained at 50°C for three days in order to dry the composite by solvent evaporation

method. After drying, the thick films of the prepared composite material were peeled off from the glass petridishes and stored in a desiccator for further studies. The *FL* is calculated by using the Eq. (1), which follows.

$$FL(wt\ \%) = \frac{M_f}{M_f + M_p} \times 100 \quad (1)$$

In Eq. (1), M_f and $M_p$denote the masses of the filler (titania NPs) and the polymer (PAM), respectively.

B. Methods

SEM images, along with energy dispersive x-ray spectrometry (EDS) spectra were obtained using Nova NanoSEM, a field emission scanning electron microscope (FE-SEM) coupled with EDAX instrumentation. Optical spectra have been recorded using Hitachi U 3310 UV-Vis-NIR spectrometer, in wavelength range varying from 190 up to 1000 nm at 25˚C. TA instruments DSC Q20 V24.10 Build 122 (from TA instrument, USA) was used to record DSC curves, for temperatures varying from 30°C up to 450°C. SDT Q 600 (TA Instruments, USA) is used to record TG-DTA thermo grams with respect to temperature, from room temperature (30°C) up to 650°C at a constant heating rate of 10°C/min, in nitrogen atmosphere.Temperature dependent DC electrical measurements for pure PAM and TiO_2 NP filled PAM composite were carried out using a research grade two probe set up which consisted of a PID controlled oven (model: PID-200), high voltage power supply (model: EHT-11) and a digital picoammeter (model: DPM-111) (purchased from SES Instruments Pvt. Ltd. Roorkee, India).

III. RESULTS AND DISCUSSIONS

A. EDS Analysis

Fig. 1 represents the EDS spectra with SEM images in the inset figure (see Fig. 1) for pure PAM and TiO_2 NP filled PAM composite films. The SEM images of pure PAM represent a plane homogeneous surface. At lower FLs of titania, such as 0.02 and 0.40 Wt %, a good dispersion of TiO_2 NPs showing their bead like structures dispersed homogeneously in the host polymeric matrix (PAM) is observed. However, the aggregation of TiO_2 NPs occurs at higher FLs. This aggregation of NPs is accompanied by an increase in the degree of crystallinity of the composite and it is manifested in the form of crystalline peaks corresponding to nano- TiO_2 in the XRD scans. Detailed analysis of SEM with particle size distribution and XRD results are presented elsewhere. The dispersion of TiO_2 NPs in PAM matrix has resulted in the microstructure modifications of the composite material which is manifested in the changes in the values of the electrical parameters and glass transition temperature (T_g) of these composites. Interaction between TiO_2 NPs and the polymer matrix provides an additional mechanism of ionic conductivity, which is enhanced along the NP-polymer interface. Thus, we observed a lowest activation energy (or highest ionic conductivity) for the titania filled PAM composite with FL of 0.40 wt% sample (where a good dispersion of NPs is observed) due to increase in the mobility of charge carriers.

The EDS spectra reveal the elemental constituents present in the sample for PAM and TiO_2 NPs filled composite films. This technique is also helpful to obtain qualitative information regarding the elemental constituents present on the surface of the sample. EDAX scans of PAM film show peaks due to fluorescence X-rays of C, N and O atoms present in the host polymer matrix. For the TiO_2 NP filled composite films, the fluorescence X-rays of Ti due to $K_{\alpha 1}$, $K_{\beta 1}$, $L_{\alpha 1}$ transitions are observed at energies 4.5, 4.9 and 0.45 keV, respectively. It can be seen that there is an increase in intensity of Ti peaks with increase in concentration of TiO_2 NPs. The table embedded in the EDS spetra (Fig. 1) represent the atomic percentage (At %) and weight percentage (Wt %) of the filler (Ti) on the surface of the corresponding sample, for a randomly selected spot on the surface of that sample. The Wt % of an element is the percentage of the weight of that element measured in the sample divided by the weights of all the elements present in the sample, whereas At % is the percentage of the number of atoms of a particular element, at that weight percentage, divided by the total number of atoms in the sample. These quantities represent the amount of TiO_2 NP present on the surface of the sample. The quantitative analysis of these values suggests that there is a variation in the quantities of the elements on the surface of the titania NP filled PAM films, with an increase in the FL. It can be seen that At % and Wt % of Ti increases with an increase in the FL. The values of At % and Wt % for the composite sample with FL 0.02Wt% is 0.09 and 0.02 respectively, while it has increased to a value of 9.47 and 2.84 for the composite sample with FL 2.8 Wt% and have maximum values of 32.64 and 12.19, respectively, for the composite sample with FL 19.5 Wt%. This increase in the At % and Wt % of Ti in TiO_2 NP filled PAM composite samples, with an increase in FL, indicates the formation of larger aggregates or clusters of titania on the surface of the sample, as the FL increases.

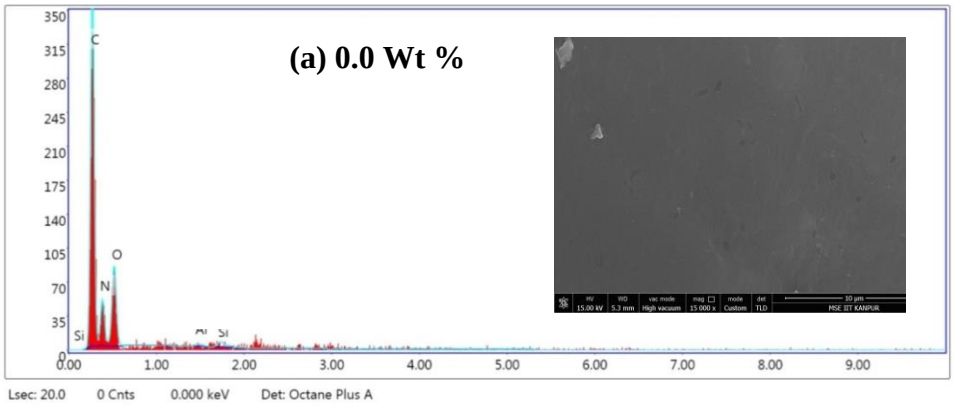
(a) 0.0 Wt %
C
O
N
Si
Lsec: 20.0 0 Cnts 0.000 keV Det: Octane Plus A

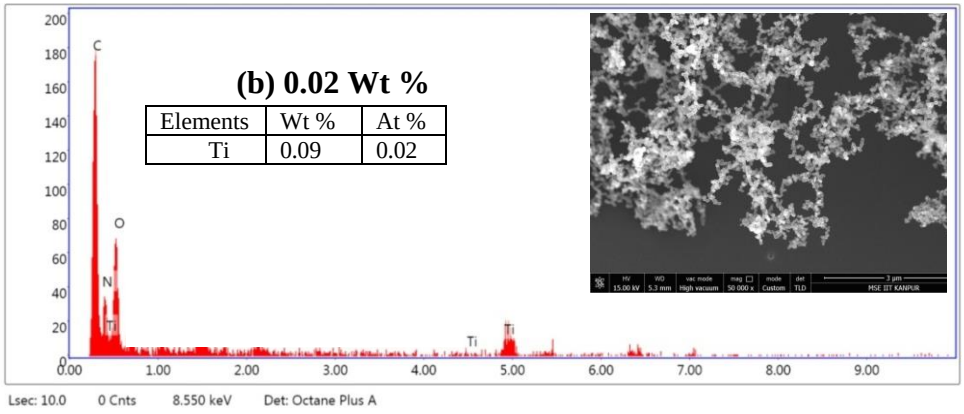
(b) 0.02 Wt %
Elements | Wt % | At %
Ti | 0.09 | 0.02
C
O
N
Ti
Lsec: 10.0 0 Cnts 8.550 keV Det: Octane Plus A

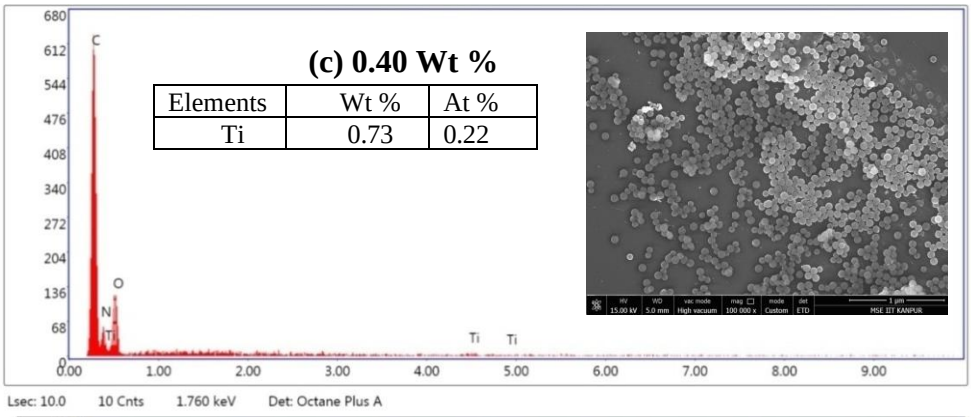
(c) 0.40 Wt %
Elements | Wt % | At %
Ti | 0.73 | 0.22
C
O
N
Ti
Lsec: 10.0 10 Cnts 1.760 keV Det: Octane Plus A

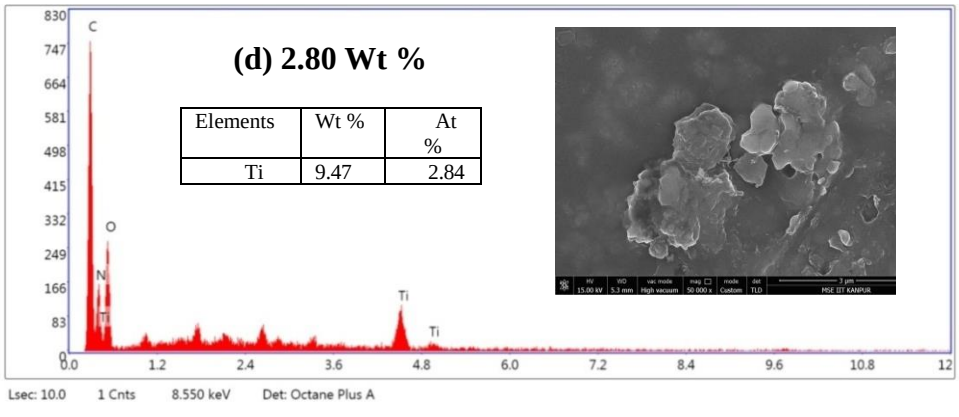
(d) 2.80 Wt %
Elements | Wt % | At %
Ti | 9.47 | 2.84
C
O
N
Ti
Lsec: 10.0 1 Cnts 8.550 keV Det: Octane Plus A

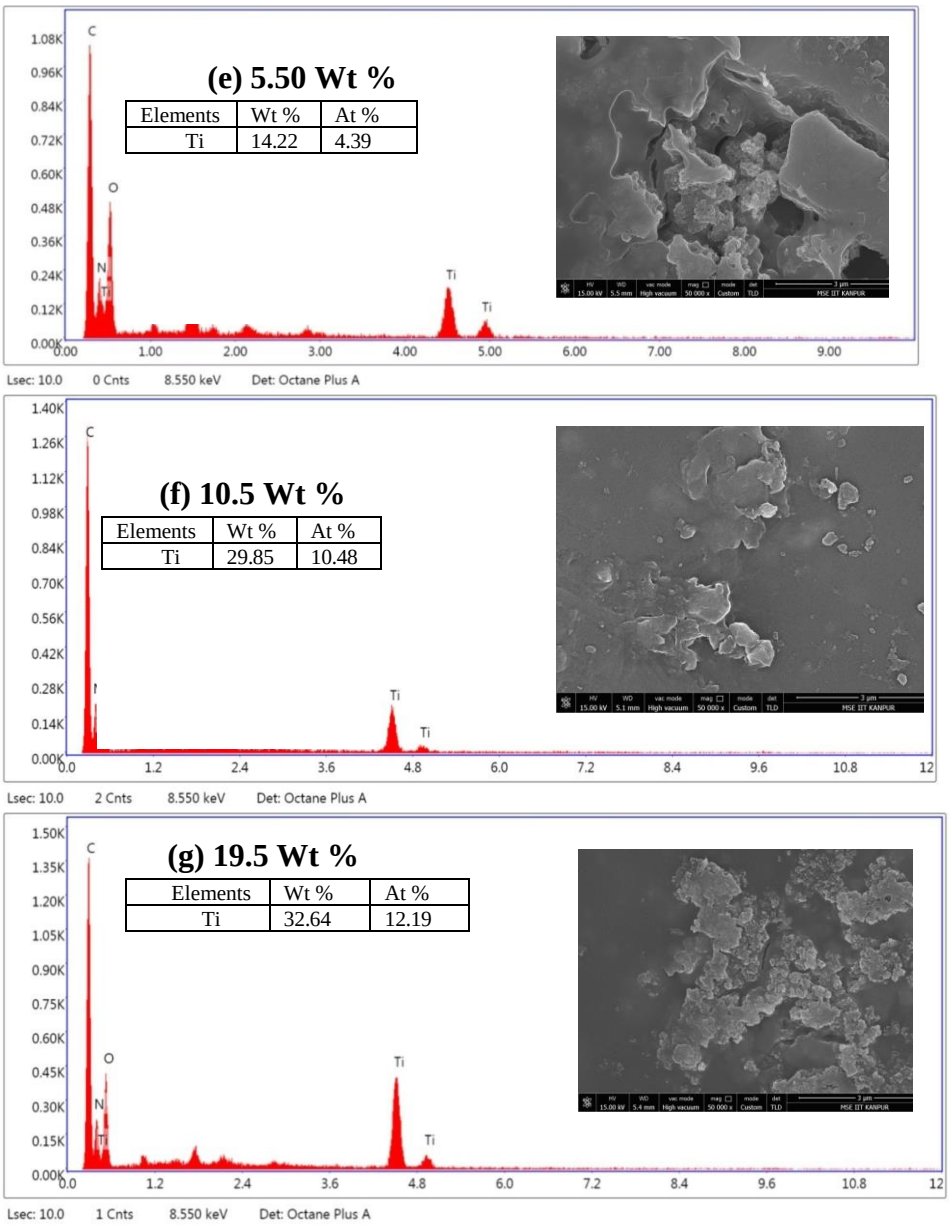

Fig. 1. EDAX images with SEM images embedded (inset) for TiO_2 NP filled PAM composite films with FLs equal to a.0.0, b. 0.02, c. 0.40, d. 2.80, e. 5.5, f. 10.5 and g.19.5 Wt. %

B. UV-Visible spectral Analysis

From the optical absorption spectra shown in Fig. 2(a), it is clear that the absorbance has increased with an increase in the FL. The major absorption band at 220 nm in pure PAM sample is attributed to the n→ π^*electronic transition. This band shifts to the region of higher wavelength for titania NP filled PAM samples. The shift of the high energy absorption edge towards longer wavelength (red shift) in the UV-Visible absorption spectra shown in Fig. 2(a) indicates that there is a decrease in the HOMO – LUMO energy gap in the prepared composite material (see Fig 2(b) as well) (Abd El-Kader et al, 2002).

A new band is observed at 345 nm in case of the TiO_2 NP filled PAM samples. This band at 345 nm corresponds to $\pi \rightarrow \pi^*$ transition. There is the emergence of a new band in the UV-Visible spectra indicating the formation of CTCs due to interaction of the added titania NPs with reactive sites in the polymer matrix (that is, molecules of PAM). Literature reveals that similar interactions were observed when nano TiO_2 was doped in PVA (Praveena et al, 2016) and when heparin calcium (Ca+) was doped in PAM matrix (Abdelrazek & Ibrahim, 2010). Addition of TiO_2 NPs into the PAM matrix results in the formation of intermediate or defect states (of varying energy) in the energy band gap of the polymer (PAM). Energy band gap

information was extracted from the absorbance spectra. Absorption coefficient (α) was determined using Eq. 2.

$$\alpha = 2.303 \times \frac{A}{d} \quad (2)$$

In Eq. 9, *A* is the normalized absorbance and *d* is the thickness of the free standing thick titania filled PAM composite film. The activation energy (E_a) for optical transitions is estimated from the slope and y-intercept of the linear portion of the plot of α versus incident photon energy (hν); the values of E_a for titania NP filled PAM films, at different FLs, are listed in Table 1.

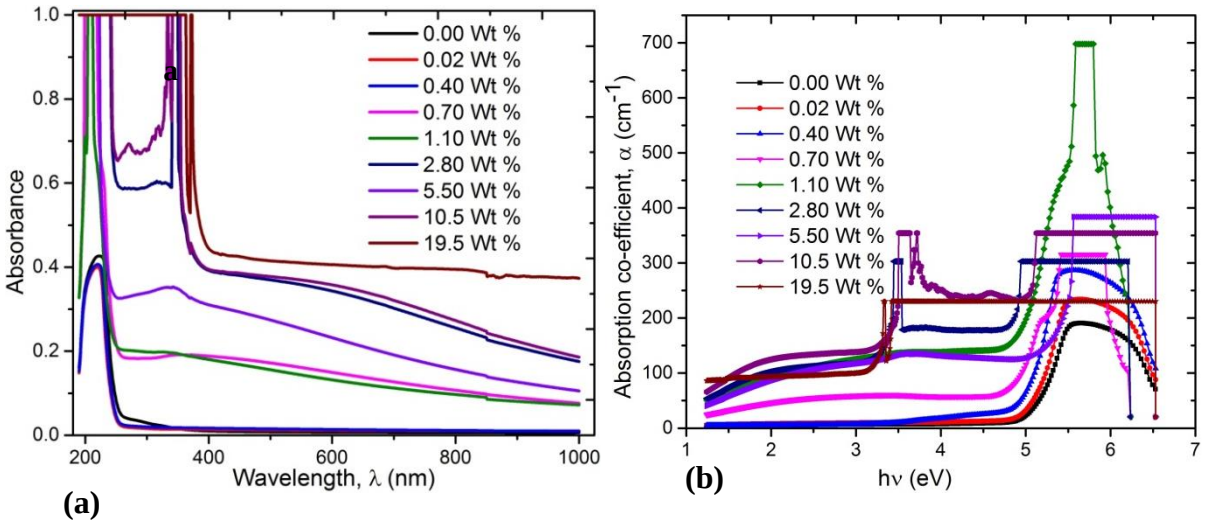

Fig. 2. (a) Plot of absorbance versus wavelength (λ) and (b) Plot of Absorption co-efficient (α) versus photon energy (hν), for pure and TiO_2 filled PAM composite films at different FLs (expressed in Wt%).

Table I.Values of activation energy (E_a) for pure PAM and TiO_2 NP filled PAM composite.

FL (Wt %)	E_a (eV) (UV-Visible)	
	E_{a1}	E_{a2}
0.00	5.39±0.04	-
0.02	5.15±0.02	-
0.40	5.07±0.06	-
0.70	5.25±0.02	4.97±0.02
1.10	5.34±0.05	-
2.80	5.01±0.07	3.48±0.05
5.50	5.43±0.03	-
10.5	5.67±0.04	3.54±0.04
19.5	5.45±0.04	3.36±0.06

C. Thermal Analysis

1) Differential Scanning Calorimetry (DSC)

DSC and TGA (along with Dr-TG) thermograms for pure PAM and TiO_2 NP filled PAM composite are shown in Fig. 3 and Fig. 4, respectively. The thermal behavior of PAM has been studied in detail by researchers (Leung et al, 1987; Van Dyke & Kasperski, 1993). Literature reports that PAM undergoes degradation in two stages (Leung et al, 1987). The pure PAM and TiO_2 NP filled PAM composite samples were subjected to a temperature program, at a steady heating rate of 10°C/min in nitrogen atmosphere. DSC scans are helpful to determine the glass transition temperature (T_g) and the onset temperature of decomposition for different decomposition stages of the composite sample. In the case of PAM and TiO_2 NP filled PAM, mass losses are observed in two significant decomposition stages; in other words, two decomposition stages are manifested as major endotherms in the DSC scans (see Fig. 3). The first endotherm below 100°C is due to loss of moisture and weakly bonded atoms (Prime, 2014; Mathot, 1994). In fact, T_g is an important physical characteristic of the amorphous polymer, which determines the temperature at which the polymer changes from glassy to rubbery state. The T_g of PAM is greatly affected by its high water retention ability. Studies reveal that, even a relatively low concentration of water in PAM acts as a plasticizer and results in lowering its T_g (Yuen et al, 1984). In the present study, the T_g values of pure PAM and TiO_2 NP filled PAM samples are found to be 140 °C and in the range 130 – 175°C, respectively. The value of T_g in case of TiO_2 NP filled PAM composites at low and moderate FLs, between 0.02 Wt% and 2.8 Wt%, is less than that of pure PAM. But at higher FLs, the value of T_g increases with increase in concentration of TiO_2 NPs (see Table 2) in the composite material. This thermal behavior of the composite material reveals that TiO_2 NPs act as plasticizer at lower FL, whereas at higher FL, the mobility of polymer chains is reduced due to increased aggregation of NPs. After crossing T_g, softening of the polymeric material is achieved, as the sample becomes rubbery. Ignoring the loss of absorbed water which takes place around 100°C, degradation of PAM and titania NP filled PAM composites can be considered to occur in two stages. The first stage of degradation starts at a temperature of 220°C, which peaks at about 260°C. There is a

second stage of sample degradation, which starts at 330°C, and this stage completes at 410°C.

Fig. 3. Thermal analysis (a) DSC thermo grams for pure PAM and TiO_2 NP filled PAM composite films.

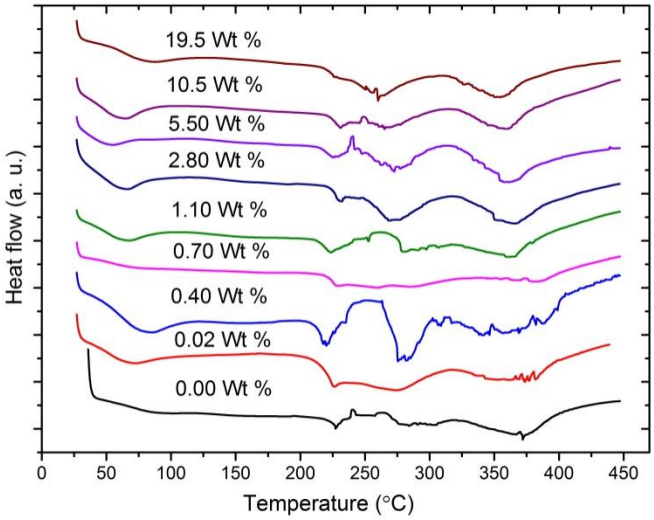

The interaction of TiO_2 NPs with PAM molecules greatly affects the chain mobility of the polymeric matrix, as witnessed through the variations in value of T_g of the composites. At lower FLs, the titania NPs do not aggregate; so, the individual NPs can easily penetrate between the polymeric chains. The large surface area of each NP allows the interaction of titania NPs with the polymeric molecules in the host matrix to form CTCs, and these NPs are responsible for lowering the degree of crystallinity of the polymeric matrix by preventing the re-crystallization of the polymeric chains. This results in the increased amorphousness of the composite sample at low FLs, which is accompanied by the lowering of T_g. The value of T_g for pure PAM and TiO_2 NP filled PAM composites are listed in Table 2. The composite with FL equal to 0.40 Wt % exhibits the lowest value of T_g (equal to 125°C). At moderate FL equal to 0.70 Wt % and 1.1 Wt %, where the aggregation of NPs has just begun, and the value of T_g has increased to 138°C and 136°C, respectively. It is to be noted that the values of T_g for these samples are still lower than that of pure PAM (140°C). With the further increase in the FL (from 2.8 Wt % up to 19.5 Wt %), aggregation of the titania NPs takes place in the host PAM matrix; these aggregates of the filler have larger size (and hence, lower surface area) when compared to the individual TiO_2 NPs. They fill up the free volume spaces in the amorphous regions of the polymeric host, thereby restricting the segmental mobility of the polymeric chains, as a result of which an increase in T_g is noted at higher FLs. The sample with FL equal to 19.5 Wt % exhibits a T_g of 174°C, which greater than that of pure PAM.

2) Thermogravimetric study

TG curves for pure PAM and TiO_2 NP filled PAM composites are shown in Fig. 4. TG curves for PAM reveal three stages of mass loss. The initial minor mass loss around 100°C is attributed to the removal of physically and chemically absorbed water and breakage of weak bonds (Leung et al, 1987; Van Dyke & Kasperski, 1993). The second stage of mass loss which occurs at temperatures varying from 210°C up to 310°C is due to the first stage of decomposition of PAM, during which release of NH_3 takes place due to imidization reactions between amide groups present in the branches of PAM (Praveena et al, 2016). The third stage of mass loss occurs at temperatures varying from 310°C up to 460°C, which is due to the second stage of decomposition of PAM; this mass loss involves the breakdown of polymer backbone and imides formed during the first decomposition stage (Abdelrazek & Ibrahim, 2010; Praveena et al, 2016). This contributes 65% of the total mass loss. Three stages of mass loss are also seen in the case of TiO_2 NP filled PAM composite samples. On incorporating TiO_2, a slight shift in the degradation temperature was observed. The shift in degradation temperature to a higher temperature (for the composite sample with FL varying from 0.02 up to 1.1 Wt %) implies an increase in thermal stability of these composites. However, for the composites with FL varying from 1.1 Wt % up to 19.5 Wt %, there is a shift in the degradation temperature to a lower temperature, and hence, there is a decrease in the thermal stability of these composites, which is attributed to the aggregation of NPs in the host polymeric material. Thermal stability of the TiO_2 NP filled PAM composites and the corresponding changes in their T_g values on incorporation of different amount of filler in the form of titania NPs into the polymer (PAM) matrix mainly depends on the degree of crystallinity, polarity, the movement of polymer chains and most importantly, on the kind of interactions taking place between the filler (titania NPs) and the polymer molecules. Literature reveals that the incorporation of TiO_2 NPs has resulted in the decrease in the value of T_g as well as an increased thermal stability in the case of different polymeric systems, which includes polypropylene, epoxy and *PVA-PVP* polymeric systems (Ramazanov et al, 2018; Kumar et al, 2016; Lobo & Veena, 2021). The results from thermal analysis are in good agreement with electrical studies (see section 3.5 for details about the electrical measurements); the decrease in the value of T_g in the case of TiO_2 NP filled PAM composites is accompanied by an increase in its electrical conductivity (and a decrease in its activation energy for thermally activated DC conduction) at low FLs of the filler in the composite. This implies that there is an increase in the availability of mobile charge carriers for electrical conduction in the composite, due to the incorporation of a small amount of TiO_2 NPs into the PAM polymer matrix.

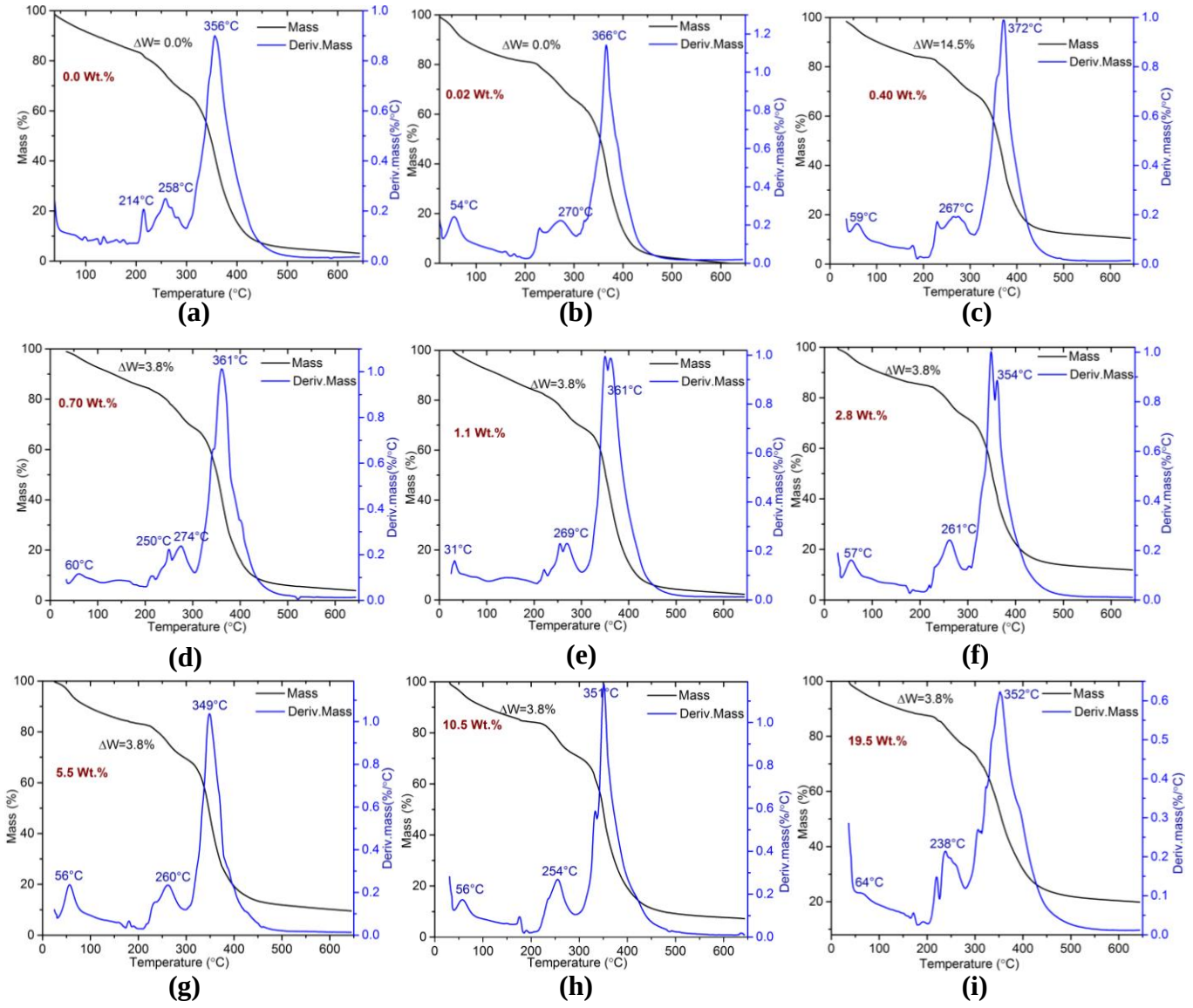

Fig. 4a-i. TG and Dr-TG thermographs for pure PAM and TiO_2 NP filled PAM composites.

Table II Onset **$T_i$ons,** Peak **T_{ip}** and Offset **$T_i$ofs** temperatures for the corresponding mass loss **ΔW_1** for PAM and TiO_2 filled PAM composite. The last column lists the glass transition temperature (T_g), expressed in degree Celsius.

FL	T_{1ons} (°C)	T_{1p} (°C)	T_{1ofs} (°C)	ΔW_1 (%)	T_{2ons} (°C)	T_{2p} (°C)	T_{2ofs} (°C)	ΔW_2 (%)	T_g (°C)
0.00	226	258	297	18.0	301	352	455	60.20	140
0.02	240	272	303	12.0	309	367	427	58.65	136
0.40	210	267	304	11.0	308	372	431	53.50	125
0.70	223	274	304	13.0	306	361	447	58.90	138
1.10	229	269	295	10.5	301	361	460	65.10	136
2.80	222	261	293	11.8	307	357	465	57.10	175
5.50	240	260	296	10.1	300	349	170	57.75	138
10.5	216	254	288	12.1	290	351	465	63.04	154
19.5	226	238	278	9.0	280	352	564	55.60	174

D. Analysis of DC electrical measurements using Variable Range Hopping (VRH) model

Electrical conductivity of pure PAM and TiO_2 NP filled PAM with an increase in temperature is due to the thermally stimulated charge carriers. This is due to the fact that the increase in temperature results in an increase in the segmental mobility of the polymeric chains which enhances the electrical conductivity. Improved conductivity in PAM filled TiO_2 NP composite samples have been observed at low FLs. This is due to the disordered states or localized states introduced by the incorporation of TiO_2 NPs in the PAM matrix, which helps in the destruction of crystalline phases of the polymer matrix and helps to enhance the amorphous regions. At low temperatures, the hopping of charge carriers (between conductive regions in the sample) takes place among the localized sites, by phonon assisted hopping. Temperature variation of electrical conductivity data for TiO_2 NP filled PAM composite is found to obey the three dimensional Variable Range Hopping (VRH) model and Mott-Davis equation (Nazeer et al, 2005; Mott & Davis E A, 1979). The data gave best fit for temperature ($T^{-1/4}$) dependence of electrical conductivity (see Fig. 5).

The Equation relating the electrical conductivity and temperature, for three dimensional VRH model is given by the following equation (see Eq. (3)).

$$\sigma T^{\frac{1}{2}} = \sigma_O \mathrm{EXP}\{-\left[\frac{T_O}{T}\right]^{\gamma}\} \quad (3)$$

In Eq. 3, σ is the DC electrical conductivity, T_o is the absolute temperature, T is temperature in Kelvin, $\gamma = \frac{1}{D+1}$ (D is the dimension) and D takes the value of 1/2, 1/3 and ¼ for 1D, 2D and 3D variable range hopping of carriers, respectively, σ_O is the pre exponential factor, with unit $Sm^{-1}K^{1/2}$ and is given by,

$$\sigma_O = \left(\frac{A^2 N(E_F)}{\alpha}\right)^{\frac{1}{2}} \quad (4)$$

In Eq. (4), N (E_F) is the density of states, α is the wave function decay constant and A is a complex parameter, expressed in $C^2s^{-1}eV^{-1/2}K^{1/2}$ and is given by,

$$A = \left(\frac{3e^2\nu_{ph}}{\sqrt{8\pi K_B}}\right) \quad (5)$$

In Eq. (5), e is the charge of electron, with value 1.602×10^{-19}C, ν_{ph} is the phonon frequency (10^{13} Hz), k_B is the Boltzmann constant and has the value 8.615×10^{-5} eVK^{-1}.

T_o is the characteristic temperature expressed in K and is given by Eq. (6).

$$T_o = \frac{16\,\alpha^3}{K\,N(E_F)} \quad (6)$$

T_o is calculated assuming the value of localization decay constant (α^{-1}) to be 3Å.

Activation energy E_a by VRH model, expressed in eV is given as,

$$E_a = \gamma\, K_B T_O \left(\frac{T_O}{T}\right)^{\gamma-1} \quad (7)$$

Activation energy is determined by substituting the value of T_o obtained from Eq. (6) in Eq. (7). Activation energy has been calculated for temperatures in the range varying from 303K up to 318 K. These values are averaged to obtain$< E_a >$.

Range of hopping (R_{hop}) in nm is determined by using the Eq. (8)

$$R_{hop} = \frac{3}{8}\left(\frac{T_O}{T}\right)^{\frac{1}{4}} \alpha^{-1} \quad (8)$$

Energy of hopping (W_{hop}) expressed in eV, is determined using the Eq. (9).

$$W_{hop} = K_B (T_O T^3)^{\frac{1}{4}} \quad (9)$$

R_{hop} and W_{hop} are calculated for a range of temperatures (T) and averaged to obtain $<R_{hop}>$ and $<W_{hop}>$, respectively.Different parameters determined by VRH model are listed in Table 3. From Table 3, we see that, the values of $< W_{hop} >$ and $< R_{hop} >$ have lower values compared to those of pure PAM at low FL (say upto 1.1 Wt. %), and these values have increased at higher FLs. This signifies that, at these lower FLs, less energy is required to overcome the barrier caused by the formation nano and micro structures in the composite material. The samples with FL 0.02 and 0.40 Wt % exhibited the lowest values of these parameters ($< W_{hop} >$ and $< R_{hop} >$) due to enhancement in the electrical conductivity of these samples caused by the uniform distribution the titania NPs in the polymer (PAM) matrix. This is also evidenced by an decrease in the value of $< E_a >$ and therefore, an increase in the value of electrical conductivity is observed. At higher FLs, a increase in $< W_{hop} >$ and $< R_{hop} >$ is observed accompanied by higher values of$< E_a >$. Thus, a decrease in electrical conductivity is observed for the titania filled PAM composite samples at higher FL.

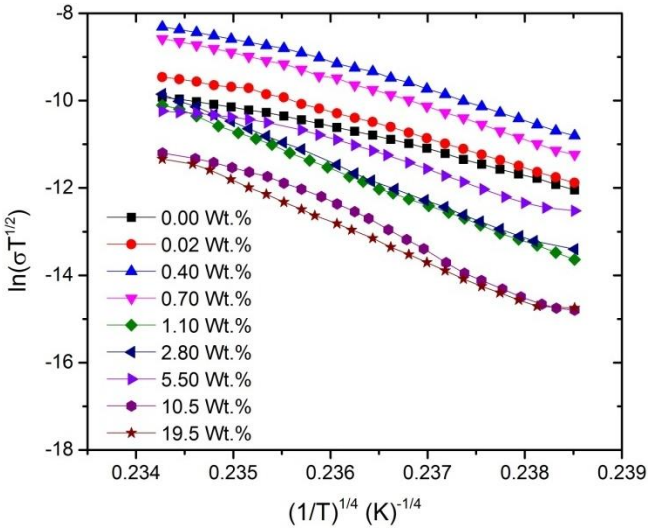

Fig. 5. Plot of $\ln(\sigma t^{1/2})$ versus $(1/T)^{1/4}$ for PAM and tio_2 nps filled PAM composite films.

Table III Activation energy determined from temperature dependence of DC conductivity; the electrical parameters determined from VRH model

FL (Wt%)	Parameters determined from Variable Rang Hopping (VRH) Model.				
	T_0 ($x10^{11}$ K)	$N(E_F)$ (x 10^{21} $eV^{-1}m^{-3}$)	$<R_{hop}>$ (nm)	$<W_{hop}>$ (eV)	$< E_a >$ (eV)
0.00	4.93	13.91	22.35	5.41	1.27
0.02	2.21	30.9	18.29	4.42	1.10
0.40	1.09	42.80	15.33	3.70	0.96
0.70	2.48	27.6	18.86	4.52	1.13
1.1	2.49	27.50	18.83	4.57	1.19
2.8	5.08	13.48	22.64	5.36	1.14
5.5	5.72	11.97	23.09	5.69	1.26
10.5	7.45	9.19	26.73	6.57	1.46
19.5	14.6	4.69	26.87	6.46	1.61

for titania filled PAM composite samples are also listed.

IV. CONCLUSIONS

Thermal, electrical and spectroscopic properties of TiO_2 NP filled PAM composite films which have been prepared using a simple solution casting technique were studied experimentally. The values of activation energy for the prepared composite films were obtained using the three dimensional VRH model. Mott's parameters were determined for TiO_2 NP filled PAM composite films from the VRH model. EDS analysis revealed the elemental constituents present in the composite samples and provided evidence for the formation of filler aggregates on the surface of the composite films. The glass transition temperature was found to decrease and thermal stability of the composite was found to increase for the composite with FL 0.40 Wt %. The enhancement in the electrical and thermal properties of this composite material at low FLs (0.02 and 0.4 Wt %) is attributed to the uniform dispersion of TiO_2 NPs in the host polymer (PAA) at these low FLs.

ACKNOWLEDGEMENTS

The authors acknowledge that the SEM images along with EDS were recorded at Indian Institute of Technology (IIT), Kanpur, respectively. The facilities at University Science Instrument Centre (USIC) and DST-SAIF, Karnatak University, Dharwad (KUD) have been used for recording the DSC and TGA spectrograms.First author acknowledges the receipt of RGNF fellowship from UGC, India.

REFERENCES

Abdelrazek, E.M., & Ibrahim, H., (2010). Effect of heparin calcium different concentrations on some physical properties and structure in polyacrylamide matrix. *Physica B*, 405(20), 4339-4343. https://doi.org/10.1016/j.physb.2010.07.038

Abd El-Kader, K. A. M., & Abdel Hamied, S. F., (2002). Preparation of poly(vinyl alcohol) films with promising physical properties in comparison with commercial polyethylene film. *Journal of Applied Polymer Science* 86(5), 1219-1226 https://doi.org/10.1002/app.11068

Ahmad, J., Deshmukh, K. & Hägg, M. B., (2013).Influence of TiO_2 on the chemical, mechanical, and gas separation properties of Polyvinyl alcohol-Titanium dioxide (PVA-TiO_2) Nanocomposite membranes.. *International. Journal of Polymer Analysis and Characterisation* 18(4), 287-296. https://doi.org/10.1080/1023666X.2013.767080

Awad, S., El-Gamal, S., El Sayed, A. M., & Abdel-Hady, E. E., (2020). Characterization, optical, and nanoscale free volume properties of Na-CMC/PAM/CNT nanocomposites. *Polymer for Advanced Technologies*, 31(1), 114-125. https://doi.org/10.1002/pat.4753

Ayanoğlu, Z. G. & Doğan, M. (2020). Characterization and thermal kinetic analysis of PMMA/modified-MWCNT nanocomposites. *Diamond and related materials*,108, 107950. https://doi.org/10.1016/j.diamond.2020.107950

Bai, J., Li, Y., Du, J., Wang. S., Zheng, J., Yang, Q., & Chen, X., (2007). One pot synthesis of polyacrylamide-gold nanocomposite. *Materials Chemistry and Physics* 106(2-3), 412-415. https://doi.org/10.1016/j.matchemphys.2007.06.021

Bahuleyan, B. K., Induja, C., & Ramesan, M. T., (2019). Influence of titanium dioxide nanoparticles on the structural, thermal, electrical properties, and gas sensing behavior of polyaniline/phenothiazine blend nanocomposites. *Polymer Composites*, 40(11), 4416-4426. https://doi.org/10.1002/pc.25303

Choudhary, P., Maurya, D. K., Tripathi, R. K., Yadav, B. C., Golubeva, N. D., Knerelman, E. I., Uflyand, I. E. & Dzhardimalieva, G. I., (2020). The synthesis of a $Cu_{0.8}Zn_{0.2}Sb_2$–polyacrylamide nanocomposite by frontal polymerization for moisture and photodetection performance. *Materials Advances* 1, 2804-2817. https://doi.org/10.1039/D0MA00389A

Dhatarwal, P., & Sengwa, R. J., (2020). Tunable β-phase crystals, degree of crystallinity, and dielectric properties of three-phase PVDF/PEO/SiO_2 hybrid polymer nanocomposites. *Materials Research Bulletin* 129, 110901. https://doi.org/10.1016/j.materresbull.2020.110901

Faupel, F., Zaporojtchenko, V., Strunskus, T., & Elbahri, M., (2010). Metal-polymer nanocomposites for functional applications. *Advanced Engineering Materials*, 12(12), 1177-1190. https://doi.org/10.1002/adem.201000231

Gavrilin, M. V., (2001). Application of Polymers & Copolymers Based on Acrylic Acid and Ethylene Oxide in Pharmacy (A Review). *Pharmaceutical Chemistry Journal*, 35, 35-39. http://dx.doi.org/10.1023/A:1010402826818

Ghosh, T. B., Dhabal, S., & Datta, A. K., (2003). On crystallite size dependence of phase stability of nanocrystalline TiO2. *Journal of Applied Physics*, 94(7), 4577. https://doi.org/10.1063/1.1604966

Green, V. S., Scott, D. E., Norton, L. D. & Graveel, J. G., (2000). Polyacrylamide molecular weight and charge effects on infiltration under simulated rainfall. *Soil Science Society of America Journal*, 64(5), 1786. https://doi.org/10.2136/sssaj2000.6451786x

Günes, S., Marjanovic, N., Nedeljkovic, J. M., & Sariciftci, N. S., (2008). Photovoltaic characterization of hybrid solar cells

using surface modified TiO_2 nanoparticles and poly(3-hexyl)thiophene. *Nanotechnology* 19(42), 424009. https://doi.org/10.1088/0957-4484/19/42/424009

Harb, V., Trentin, A., Uvida, M. C., Magnani, M., Pulcinelli, S. H., Santilli, C. V., & Hammer, P., (2020). A comparative studyon PMMA-TiO_2 and PMMA-ZrO_2 protective coating. *Progress in Organic Coatings* 140, 105477. https://doi.org/10.1016/j.porgcoat.2019.105477

Hari, M., Joseph, A., Mathew, S., Radhakrishnan, P., & Nampoori, V. P. N., (2012). Band-gap tuning and nonlinear optical characterization of Ag: TiO2 nanocomposites. *Journal of Applied Physics* 112, 074307. https://doi.org/10.1063/1.4757025

Hassan, T., Salam, A., Khan, A., Khan, S. U., Khanzada, H., Wasim, M., Khan, M. Q., & Kim, I. S., (2021). Functional nanocomposites and their potential applications: A review. *Journal of Polymer Research* 28, 36. https://doi.org/10.1007/s10965-021-02408-1

Huyen, D. N., Tung, N. T., Thien, N. D., & Thanh, L. H., (2011).Effect of TiO_2 on the gas sensing features of TiO_2/PANi nanocomposites. *Sensors* 11(2), 1924-1931. https://doi.org/10.3390/s110201924

Kim, D. J., Jo, M. J., & Nam, S. Y., (2015). A review of polymer-nanocomposite electrolyte membranes for fuel cell application. *Journal of industrial and engineering chemistry*, 21**,** 36-52. https://doi.org/10.1016/j.jiec.2014.04.030

Kumar, K., Ghosh, P. K. & Kumar, A., (2016). Improving mechanical and thermal properties of TiO_2-epoxy nanocomposite. *CompositesPart B: Engineering* 97:353-360. https://doi.org/10.1016/j.compositesb.2016.04.080

Leung, W. M., Axelson, D. E. & Van Dyke, J. D., (1987). Thermal degradation of polyacrylamide and poly(acrylamide-co-acrylate). *Journal of Polymer Science.A:Polymer Chemistry*, 25(7):1825-1846. https://doi.org/10.1002/pola.1987.080250711

Liu, T., Chen, X., Tervoort, E., Kraus, T., & Niederberger, M., (2021). Desigh and fabrication of transparent and stretchable Zinc ion batteries. *ACS Applied Energy Materials*,4(6), 6166-6179. .https://doi.org/10.1021/acsaem.1c00958

Li, H., Liu, F., Fan, B. Y., Ai, D., Peng, Z. & Wang, Q., (2018). Nanostructued ferroelectric-polymer composites for capacitive energy stirage. *Small Methods*, 2(6), 1700399. https://doi.org/10.1002/smtd.201700399

Lobo, B. & Veena, G., (2021). Experimental investigations on nano-titania incorporated polyvinyl alcohol- polyvinyl pyrrolidone composite films. *Polymer-Plastics technology and materials.* 60(15),1697-1717. https://doi.org/10.1080/25740881.2021.1930045

Mai, Y-W. & Yu, Z-Z., (2006). Polymer Nanocomposites. WoodHead publishing limited, Cambridge, England.

Mathot, V. B. H., (1994). Calorimetry and thermal analysis of polymers. Carl Hanser Verlag GmbH and Co,Munich, Germany, New York.

Mott, N. F., & Davis, E. A., (1979) *Electronic processes in Noncrystalline Materials.* 2nd ed. (Oxford University Press) ISBN: 9780199645336

Nazeer, K. P., Thamilselvan, M., Mangalaraj, D., Narayandass Sa, K., & Yi, J., (2006). Direct and High Frequency Alternating Current Conduction Mechanisms in Solution Cast Polyaniline Films. *Journal of Polymer Research*, 13, 17-23. https://doi.org/10.1007/s10965-005-9007-9

Olad, A,, Behboudi, S., & Entezami, A. A., (2012). Preparation, characterization and photocatalytic activity of TiO_2/polyaniline core-shell nanocomposite. *Bulletin of Materials Science* 35, 801-809.

Praveena, S. D., Ravindrachary, V., Bhajantri, R. F., & Ismayil (2016). Dopant-induced microstructural, optical, and electrical properties of TiO_2/PVA composite. *Polymer Composites*, 37(4), 987-997 https://doi.org/10.1002/pc.23258

Prime, R. B., (2014). Thermal analysis of polymers: Fundamentaland applications. J. D. Menczel, R. B. Prime (Editors), John Wiley and sons, Hoboken, New Jersey.

Rajeh, A., Ragab, H. M., & Abltalib, M. M., (2020). Co doped ZnO reinforced PEMA/PMMA composite: structural, thermal, dielectric and electric properties for electrochemical applications. Journal of *Molecular Structure, 1*217, 128447. https://doi.org/10.1016/j.molstruc.2020.128447

Ramazanov, M. A., Hajiyeva, F. V., & Maharramov, A. M., (2018). Structure and properties of PP/TiO_2 based polymer nanocomposites. *Integrated Ferroelectrics*, 192(1):103-112. https://doi.org/10.1080/10584587.2018.1521658

Roy, S., & Prabhakar, B., (2010). Bioadhesive polymeric platforms for transmucosal drug delivery systems-a review., *Tropical journal of pharmaceutical research*, 9, 1. https://doi.org/10.4314/tjpr.v9i1.52043

Sankar, S., Naik, A. A., Anilkumar, T. & Ramesan, M. T., (2020). Characterization, conductivity studies, dielectric properties, and gas sensing performance of in situ polymerized polyindole/copper alumina nanocomposites. *Journal of applied Polymer Science*, 137(38), 49145. https://doi.org/10.1002/app.49145

Shameem, M. M., Sasikanth, S. M., Annamalai, R., & Raman, R. G., (2021). A brief review on polymer nanocomposites and its applications. *Materials Today Proceedings.* 45(2), 2536-2539. https://doi.org/10.1016/j.matpr.2020.11.254

Shrivastava, S., Jadon, N., & Jain, R., (2016). Next-generation polymer nanocomposite-based electrochemical sensors and biosensors: A review. *TrAC Trends in Analytical Chemistry*, 82, 55-67. https://doi.org/10.1016/j.trac.2016.04.005

Shukla, P., & Saxena, P., (2021). Polymer nanocomposites in sensor applications: a review on present trends and future scope. *Chinese Journal of Polymer Science*, 39, 665-691. https://doi.org/10.1007/s10118-021-2553-8

Singh, P. K., Bhattacharya, B., & Nagarale, R. K., (2010).Effect of nano-TiO_2 dispersion on PEO polymer electrolyte property. *Journal of Polymer Science*, 118(5), 2976-2980. https://doi.org/10.1002/app.32726

Singh, S. P., Sharma, S. K., & Kim, D. Y., (2020). Carrier mechanism of ZnO nanoparticles-embedded PMMA nanocomposite organic bistable memory device. *Solid State Sciences* 99, 106046. https://doi.org/10.1016/j.solidstatesciences.2019.106046

Van Dyke, J. D., & K. L. Kasperski. 1993. Thermogravimetric study of polyacrylamide with evolved gas analysis. *Journal of Polymer Science A: Polymer Chemistry*, 31(7),1807-1823. https://doi.org/10.1002/pola.1993.080310720

Virya, A., & Lian, K., (2017). Polyacrylamide-lithium chloride polymer electrolyte and its applications in electrochemical

capacitors. *Electrochemistry Communications* 74, 33-37. https://doi.org/10.1016/j.elecom.2016.11.014

Wang, Z., Bockstaller, M. R., & Matyjaszewski, K., (2021). Synthesis and applications of ZnO/Polymer nanohybrids. *ACS Materials Letter* 3(5), 599-621. https://doi.org/10.1021/acsmaterialslett.1c00145

Wever, D. A., Picchioni, F., & Broekhuis, A. A., (2013). Branched polyacrylamides: Synthesis and effect of molecular architecture on solution rheology. *European Polymer Journal*, 49(10), 3289-3301. http://dx.doi.org/10.1016%2Fj.eurpolymj.2013.06.036

Xie, H., Yu, Q., Mao, J., Wang, S., Hu, Y., & Guo, Z., (2020). A conductive polyacrylamide/double bond chitosan/polyaniline hydrogel for flexible sensing. *Journal of Materials Science: Materials in Electronics*, 31(13), 10381-10389.

Yuen, H. K., Tam, E. P. & Bulock, J. W. (1984). On the Glass Transition of Polyacrylamide. In: Johnson J.F., Gill P.S. (eds) Analytical Calorimetry. Springer, Boston, MA. https://doi.org/10.1007/978-1-4613-2699-1_2

Zhou, L., & Jiang, Y. F., (2020).Recent progress in dielectric nanocomposites. *Materials Science and Technology*, 36(1). https://doi.org/10.1080/02670836.2019.1675335

Zhao, X-Y, & Liu, H-J., (2010). Review of Polymer materials with low dielectric constant. *Polymer international*, 59(597), 597-606. https://doi.org/10.1002/pi.2809

Zulkifli, A., (2012). Polymer dielectric materials. *IntechOpen.* http://dx.doi.org/10.5772/50638

***